NASA CR-

Equivalent gravity modes -- an interim evaluation

Richard S. Lindzen[1]

and

Siu-shung Hong

(NASA-CR-132779) EQUIVALENT GRAVITY MODES - AN INTERIM EVALUATION (Chicago Univ.) 29 p HC $3.50 CSCL 04A
N73-26383
Unclas
G3/13 08476

University of Chicago

January 1972

[1] Alfred P. Sloan Foundation Fellow

Abstract

The behavior of the main solar semidiurnal tidal mode in a dissipative atmosphere is studied both in a rotating spherical atmosphere and by means of the equivalent gravity mode approximation. The former involves the numerical solution of a two dimensional partial differential equation which (due to the presence of friction) is non-separable. The latter involves approximating the tidal mode at the equator by means of an internal gravity wave on a non-rotating plane; this approximation has been used extensively in earlier studies of the behavior of atmospheric tides in the thermosphere where viscosity assumes dominant importance. In the present study, dissipation is modelled by Newtonian cooling and Rayleigh friction, both of which are taken to increase inversely with mean density. Coefficients are chosen to crudely simulate the effects of molecular viscosity and conducitivity. The results of this study provide an opportunity to evaluate the equivalent gravity mode formalism. Our main findings are:

i) Below 130 km, where friction is unimportant, equivalent gravity mode results are, for all practical purposes, identical to those at the equator obtained from a spherical calculation.

ii) Above 130 km amplitudes over the equator obtained from the spherical calculation are about 30% smaller than those obtained from the equivalent gravity mode calculations. Also, there is a 15° (1/2 hour) difference in phase.

iii) The amplitude reduction over the equator, cited above, is associated with a broadening of the latitude distribution of amplitude for the oscillatory pressure and temperature fields within the thermosphere. There is also a significant variation of phase with latitude within the thermosphere. Associated with the above variations are significant changes in the latitude distribution of h orizontal velocity within the thermosphere.

Equivalent Gravity Modes -- an interim evaluation

1. Introduction.

The solution of the problem of linearized internal waves (including tides) in an otherwise static atmosphere with friction on a rotating sphere is rendered especially difficult, because the joint presence of friction, rotation and sphericity lead to a mathematical problem in which altitude and latitude dependence are no longer separable (Chapman and Lindzen, 1970). Furthermore, when the friction is due in significant measure to the presence of molecular viscosity (as is the case in the thermosphere) the resulting equation is of eighth order in altitude. Yet, the solution of this problem is of substantial importance since within the thermosphere, where tides virtually dominate the meteorology, we have a transition from essentially inviscid solutions to solutions dominated by friction; the behavior in the latter region is, significantly, determined by the complicated transition region.

In order to obtain some insight into the above problem without tackling the non-separability I developed what I called the equivalent gravity mode formalism (Lindzen, 1970; 1971; Lindzen and Blake, 1971). This formalism exploited the following facts:

i) In the absence of friction the linearized equations for internal waves in an otherwise static atmosphere on a rotating sphere are separable in their horizontal and vertical dependences; the same is true on a rotating (or non-rotating) plane. The horizontal geometry and the rotation affect the separation constants (known as equivalent depths, viz., Lindzen, 1970) which in turn determine the vertical structure. However, for the same equivalent depths one will get the same vertical structure regardless of the horizontal geometry or rotation.

ii) As a corollary to the above consider a planar, nonrotating frictionless atmosphere where quite arbitrarily we identify one horizontal direction with the North-South direction and the other with the East-West direction. For any internal mode (whether tidal or not) in a spherical rotating frictionless atmosphere, there exists a mode in the nonrotating planar atmosphere which, through appropriate choice of North-South wavenumber, will have the same East-West wavenumber obtaining on the sphere at the equator, as well as the same period and vertical structure as the spherical mode.

iii) The effects of friction are to a large extent determined by the ratio of dissipative time scale to wave period.

iv) On a nonrotating plane the frictional problem is separable.

The equivalent gravity mode formalism consists in taking a wave as described in item (ii) above and matching it to a tidal mode in a rotating spherical atmosphere. One then examines the behavior of the planar mode in an atmosphere whose vertical distributions of mean temperature and friction (viscosity and ion drag) match those of the earth's atmosphere. It was argued that the results should approximate those obtained at the equator in a full calculation on a rotating sphere.

The problem for a rotating sphere results from the fact that latitudinal structure of a given tidal mode will change with altitude when friction becomes comparably important with the coriolis force; the changing latitudinal structure can then produce modifications in vertical structure. It was felt, however, that in the neighborhood of the equator, where Coriolis terms are zero, such effects ought to be relatively small. It was shown, moreover, that oscillations within the thermosphere, excited by heating within the thermosphere, were not very sensitive to the latitude distribution of the excitation. This last finding was particularly important for diurnal oscillations in the thermosphere which it was shown would be almost entirely excited in situ. Indeed the theoretical results obtained for diurnal oscillations (Lindzen, 1971, ~~1971a~~) are reasonably compatible with observations of thermospheric daily variations.

However, the equivalent gravity mode formalism also suggests that there should be, within the thermosphere, a large semidiurnal oscillation (temperature amplitude 200°K) which propagates into the thermosphere from the mesosphere where it is excited by ultraviolet radiation absorbed by ozone. Semidiurnal oscillations of the predicted magnitude have not, as yet, been found in the available thermospheric data, and while the data are by no means certain, there is nonetheless good reason to reexamine the theory. One of the first points one might question (though hardly the only one) is the equivalent gravity mode formalism, itself. Fortunately, it is at least qualitatively possible to do this without integrating an eighth order non-separable partial differential equation. The point is that all our arguments concerning the equivalent gravity mode formalism should apply as well to an atmosphere where the friction is due to Rayleigh friction (linear drag) with a rate coefficient inversely proportional to density as to an atmosphere where friction is due to molecular viscosity. In the former case, we have only to deal with a second order non-separable partial differential equation whose numerical integration is economically feasible. It thus becomes possible to compare an equivalent gravity mode solution with an accurate numerical solution on a rotating sphere. Moreover, the height dependence of the quantity $\frac{\delta p}{p_o}$ (where δp is the pressure oscillation and p_o is the mean pressure) in an atmosphere with Rayleigh friction (and/or Newtonian cooling) increasing as $1/\rho_o$ (where ρ_o is the mean density) is similar to the behavior of the oscillatory temperature and horizontal velocity fields in an atmosphere with molecular viscosity and thermal conductivity (Lindzen, 1968). A study, therefore, of the behavior of $\frac{\delta p}{p_o}$ in the simple system may offer quantitative insight into the behavior of the more realistic system.

The study of a system with Rayleigh friction and Newtonian cooling is the purpose of this paper.

2. Equations.

For the inviscid tidal problem (see Chapman and Lindzen (1970) for derivations) one may reduce the linearized equations of motion to a single equation in a single unknown. A convenient choice for the unknown is

$$G = -\frac{1}{\gamma p_0}\frac{Dp}{Dt} \qquad (1$$

where $\gamma = c_p/c_v = 1.4$

$$\frac{Dp}{Dt} = \frac{\partial \delta p}{\partial t} + w\frac{dp_0}{dz}$$

t = time, z = altitude, p = pressure, p_0 = mean pressure and δp = tidal pressure perturbation. The equation for G is

$$H\frac{\partial^2 G}{\partial z^2} + \left(\frac{dH}{dz} - 1\right)\frac{\partial G}{\partial z} = \frac{g}{4r^2\omega^2}F\left[\left(\frac{dH}{dz} + \kappa\right)G - \frac{\kappa J}{\gamma g H}\right] \qquad (2$$

where J is the tidal heating per unit mass and time,

$$F \equiv \frac{1}{\sin\theta}\frac{\partial}{\partial\theta}\left(\frac{\sin\theta}{f^2-\cos^2\theta}\frac{\partial}{\partial\theta}\right) - \frac{1}{f^2-\cos^2\theta}\left(\frac{s}{f}\frac{f^2+\cos^2\theta}{f^2-\cos^2\theta} + \frac{s^2}{\sin^2\theta}\right),$$

$f = \sigma/2\omega$; θ is the colatitude, s the zonal number of wave, $\kappa = \frac{\gamma-1}{\gamma}$, g = acceleration of gravity, $H = RT_0/g$ = local scale height, σ Y tidal frequency, ω = earth's rotation rate and r = earth's radius, and T_0 = basic temperature. Equ. (2) may be solved by separation of variables. The resulting equations for latitude dependence (Laplace's Tidal Equation) is

$$\frac{1}{\sin\Theta}\frac{\partial}{\partial\Theta}\left(\frac{\sin\Theta}{f^2-\cos^2\Theta}\frac{\partial\Theta_n}{\partial\Theta}\right)-\frac{1}{f^2-\cos^2\Theta}\left(\frac{s}{f}\frac{f^2+\cos^2\Theta}{f^2-\cos^2\Theta}+\frac{s^2}{\sin^2\Theta}\right)\Theta_n \quad (3$$

$$= -\frac{4r^2\omega^2}{g h_n}\Theta_n$$

where hn is the separation constant and we have assumed

$$G = \sum_n G_n(z)\,\Theta_n \quad .$$

Equ. (3) with the requirement of boundedness at the poles forms an eigenfunction-eigenvalue problem for $\{\Theta_n\}$ and $\{h_n\}$.

If we expand J in terms of (3)'s eigenfunctions (Hough functions); i. e.,

$$J = \sum_n J_n(z)\,\Theta_n(\Theta),$$

then the equation for the vertical structure of the n^{th} mode is

$$H\frac{d^2G_n}{dz^2}+\left(\frac{dH}{dz}-1\right)\frac{dG_n}{dz}+\frac{1}{h_n}\left(\frac{dH}{dz}+\kappa\right)G_n = \frac{\kappa J_n}{\gamma g h_n H} \quad (4$$

The boundary conditions for (4) are

$$H\frac{dG_n}{dz}+\left(\frac{H}{h_n}-1\right)G_n = 0 \qquad \text{at } z = 0$$

(derived from the requirement $w = 0$ at $z = 0$), and that no energy be received from ∞. For waves on a planar, nonrotating atmosphere, (3) is replaced by a trivial equation for which one has solutions of the following form

$$\Theta_n = e^{ikx}\begin{cases}\cos my & m^2>0\\ \cosh my & m^2<0\end{cases} \quad (5$$

where K corresponds to a zonal wavenumber, m corresponds to a latitude wavenumber and

$$h_m = \frac{\sigma^2/g}{K^2 + m^2} . \qquad (6$$

It proves useful to allow m to be non-integral. The equation for vertical structure remains identical to (4). This forms the basis for the equivalent gravity mode formalism. The equivalent gravity wave being a wave for which σ is equal to that of a tidal mode, $K = \frac{s}{r}$ (the spherical mode's zonal wavenumber at the equator), and m is chosen so that h equals the equivalent depth of the corresponding spherical mode. The resulting gravity wave will have the same vertical structure as the spherical mode (Lindzen and Blake, 1971). Moreover the gravity wave fields are asymptotic to the spherical solutions as one approaches the equator. The assumption of the equivalent gravity mode formalism is that the last feature remains approximately true in the presence of friction. The extent to which the approximation holds, however, still has not been securely determined.

To make the problem clearer we shall explicitly introduce Rayleigh friction and Newtonian cooling. These enter the equations of horizontal momentum and energy as follows:

$$\frac{\partial u}{\partial t} - 2\omega v \cos\theta = -\frac{1}{r}\frac{\partial}{\partial\theta}\left(\frac{\delta p}{\rho_0}\right) - \nu u \qquad (7$$

$$\frac{\partial v}{\partial t} + 2\omega u \cos\theta = -\frac{1}{r\sin\theta}\frac{\partial}{\partial\varphi}\left(\frac{\delta p}{\rho_o}\right) - \nu v \qquad (8$$

$$\frac{\partial \delta T}{\partial t} + a\,\delta T + w\frac{dT_o}{dz} = \frac{(\gamma-1)}{R}\frac{gH}{\rho_o}\left(\frac{\partial \delta p}{\partial t} + w\frac{dp_o}{dz}\right) + \frac{\gamma-1}{R}J \qquad (9$$

where ν, a are the Rayleigh friction and Newtonian cooling coefficients, respectively; u the northerly, v the westerly wind velocities and δT the temperature; ρ_o is the mean density distribution.

In terms of the geopotential (or, more precisely, $\delta p/\rho_o$), the final equation is

$$\frac{\partial^2}{\partial z^2}\left(\frac{\delta p}{\rho_o}\right) - \left\{\frac{1}{H} + \frac{a}{i\sigma\gamma}\left(1+\frac{a}{i\sigma\gamma}\right)^{-1}\frac{1}{H}\frac{dH}{dz} + \left(1+\frac{a}{i\sigma\gamma}\right)^{-1}\frac{d}{dz}\left(\frac{a}{i\sigma\gamma}\right) + \left(K+\frac{dH}{dz}\right)^{-1}\frac{d^2H}{dz^2}\right\}\frac{\partial}{\partial z}\left(\frac{\delta p}{\rho_o}\right) - \frac{g}{4\omega^2 r^2}\frac{1}{H}\left(K+\frac{dH}{dz}\right)\left(1+\frac{\nu}{i\sigma}\right)\left(1+\frac{a}{i\sigma\gamma}\right)^{-1}\hat{F}\left(\frac{\delta p}{\rho_o}\right)$$

$$+\frac{a}{i\sigma\gamma}\left(1+\frac{a}{i\sigma\gamma}\right)^{-1}\left\{\frac{1}{H^2}\frac{dH}{dz}\left(1+\frac{dH}{dz}\right) - \frac{1}{H}\frac{dH}{dz}\left(\frac{1}{a}\frac{da}{dz}\right) - \frac{K}{H}\left(K+\frac{dH}{dz}\right)^{-1}\frac{d^2H}{dz^2}\right\}\cdot\left(\frac{\delta p}{\rho_o}\right)$$

$$= \left(1+\frac{a}{i\sigma\gamma}\right)^{-1}\frac{1}{H}\frac{\partial}{\partial z}\left(\frac{KJ}{i\sigma}\right) - \left(1+\frac{a}{i\sigma\gamma}\right)^{-1}\frac{1}{H}\left[\left(K+\frac{dH}{dz}\right)^{-1}\frac{d^2H}{dz^2} + \frac{1}{H}\left(1+\frac{dH}{dz}\right)\right]\left(\frac{KJ}{i\sigma}\right) \qquad (10$$

where

$$\hat{F} = \frac{1}{\sin\theta}\frac{\partial}{r\partial\theta}\left(\frac{\sin\theta}{\hat{f}^2-\cos^2\theta}\frac{\partial}{r\partial\theta}\right) - \frac{1}{(\hat{f}^2-\cos^2\theta)}\left\{\frac{s}{\hat{f}}\frac{(\hat{f}^2+\cos^2\theta)}{(\hat{f}^2-\cos^2\theta)} + \frac{s^2}{\sin^2\theta}\right\}$$

with $\hat{f} \equiv \frac{\sigma}{2\omega} - i\frac{\nu}{2\omega}$.

$\frac{\delta p}{p_0}$ is related to G by:

$$G=\frac{i\sigma}{g\gamma}\left(K+\frac{dH}{dz}\right)^{-1}\left\{-\left(1+\frac{a}{i\sigma\gamma}\right)\frac{\partial}{\partial z}\left(\frac{\delta p}{p_0}\right)+\frac{a}{i\sigma\gamma}\frac{1}{H}\frac{dH}{dz}\frac{\delta p}{p_0}+\frac{K}{H}\frac{J}{i\sigma}\right\}$$

Due to the joint presence of ν and ω, equ. (10) is no longer separable. It is a two-dimensional equation which must be solved numerically. On the other hand the equations for a nonrotating planar atmosphere remain separable with equs. (5) and (6) still holding. Equ. (4) becomes

$$\frac{d^2 G_m}{dz^2}-\left\{\frac{1}{H}-\left(1+\frac{a}{i\sigma\gamma}\right)^{-1}\frac{1}{H}\frac{dH}{dz}-\frac{\nu}{i\sigma}\left(1+\frac{\nu}{i\sigma}\right)^{-1}\frac{1}{\nu}\frac{d\nu}{dz}\right\}\frac{dG_m}{dz}$$

$$-\left\{-\frac{1}{H}\left[\frac{\nu}{i\sigma}\left(1+\frac{\nu}{i\sigma}\right)^{-1}\frac{1}{\nu}\frac{d\nu}{dz}-\frac{a}{i\sigma\gamma}\left(1+\frac{a}{i\sigma\gamma}\right)^{-1}\frac{1}{H}\frac{dH}{dz}\right]\right.$$

$$\left.-\frac{g}{\sigma^2 H}(m^2+k^2)\left(1+\frac{\nu}{i\sigma}\right)^{-1}\left(1+\frac{a}{i\sigma\gamma}\right)^{-1}\left(K+\frac{dH}{dz}\right)\right\}G_m$$

$$=\frac{g}{\sigma^2 H}(m^2+k^2)\left(1+\frac{\nu}{i\sigma}\right)^{-1}\left(1+\frac{a}{i\sigma\gamma}\right)^{-1}\frac{K J_m}{\gamma g H} \qquad (11$$

Equ. (11) must also be solved numerically, but it is only one-dimensional.

Our procedure will be to focus on the main symmetric semidiurnal mode for which h = 7.85 km, $\sigma = 4\pi/1$ day, and s = 2. ν and a are chosen to simulate dissipative time scales due to viscosity and conductivity; dissipative effects are, therefore, negligible below about 100 km. The explicit choice is

$$\nu = 6.214\times10^{-12}\ m^{-1}sec^{-1}\ H\exp\left(\int_0^z\frac{dz'}{H}\right)$$

where H = scale height in meters.

$$a = \gamma_4 \cdot \tilde{a}$$

$$\tilde{a} = 1.185 \times 10^{-6}\ \text{sec}^{-1}\ \exp\left(-\left(\frac{z - 50\,\text{km}}{23.25}\right)^2\right) \qquad \text{(12a, b, c}$$

'$\tilde{a}$' simulates infrared cooling (which proves to have a negligible effect on the main semidiurnal mode).

Our excitation will be due to ozone and water vapor absorption, both of which are located below 100 km. In this region, inviscid modal (Hough modes) structure is meaningful, and we, in fact, consider excitation of the form of the main semidiurnal mode; i.e., in an inviscid atmosphere only a single mode would be excited. The vertical distribution of excitation is given in Chapman and Lindzen (1970). An identical vertical distribution of excitation is used for the equivalent gravity mode (viz., Lindzen and Blake, 1971). For T_o we use the ARDC standard atmosphere. The composition of the atmosphere (and hence the gas constants) are assumed constant.

Both equations (10) and (11) are solved by the method described in Lindzen and Kuo (1970). In both instances a resolution of .5 km in the vertical is used. In both cases solutions asymptote to $G \propto e^{-x}$ as $z \to \infty$. The asymptotic regime sets on by 250 km. We therefore take $\frac{\partial G}{\partial z} = -\frac{G}{H}$ at z = 300 km. For equ. (10) we find eleven points from pole to pole to constitute adequate resolution; 21 points altered solutions by less than 5%. We will compare the spherical solution of $\delta p/p_o$ at the equator with the equivalent gravity mode solution. We will also consider the deviations of the latitude structures obtained on a sphere from those of inviscid Hough modes.

3. Results.

In Figure 1 we show the distribution with height of the amplitude and phase of $\delta p / p_0$ both for the e.g.m. calculation and at the equator for the spherical calculation. Also shown are results at the equator for a dissipationless atmosphere. The reason for showing the dissipationless results will be discussed later. Restricting ourselves to the two dissipative cases we see that there is virtually perfect agreement below about 80 km. Above 130 km noticeable differences begin to develop. Above 200 km these differences amount to about 1/2 hour (or, equivalently, 15°) in phase; amplitudes for calculations on a rotating sphere are about 30% less than those obtained from e.g.m. calculations. The latter difference is not surprising: when one has a transition from exponentially increasing amplitudes to constant amplitude with height[1], small variations in the height and nature of the transition can lead to significant amplitude differences above the transition.

Between 80 km and 130 km there are small differences between e.g.m. and spherical calculations (amounting to a few minutes of phase and a few percent in amplitude) which, while too small to be of

---

[1]This is precisely the behavior of horizontal velocity and temperature when dissipation is due to molecular viscosity and conductivity.

practical significance, appear to be real. Some idea of the origin of these small discrepancies may be obtained by comparing c.g.m. results with dissipationless results in Figure 1a. The differences below 130 km arise from the fact that dissipation varying with height can cause the reflection of internal gravity waves. This matter is reviewed in Lindzen (1970). On the other hand, below 130 km dissipationless and dissipative results for a rotating sphere are virtually identical, suggesting that the reflectivity has been substantially diminished.

A study of the variation of the semidiurnal tide with latitude, as obtained from the spherical calculation, casts some light on the results shown in Figure 1; it also shows some rather unexpected aspects of the interaction of friction and rotation in a spherical atmosphere. In Figures 2 and 3 we show, repsectively, the variation of amplitude and phase with height for $\delta p/p_0$ (i.e., the fractional variation of pressure due to the main semidiurnal mode) at different latitudes. We see in Figure 2 that the amplitude variation is similar at all latitudes for $z \lesssim 130$ km -- indicative of the fact that the tide propagates vertically without change of horizontal form. Similarly, we see in Figure 3 that the phase is independent of latitude below 130 km. These results are exactly what is obtained from inviscid theory when only the main mode is excited. However, above 130 km we see that the amplitude profiles draw closer together. More explicitly, $\left|\frac{\delta p}{p_0}\right|$ at $y = .8$ (latitude = 53.2°) increases up to 170 km, asymptoting to a constant above this height; at $y = 0$ (equator, $y = \cos 0$), on the other hand, $\left|\frac{\delta p}{p_o}\right|$ increases up to 150 km, then decreases about 30% before asymptoting to a constant above 200 km. This leads to a latitudinal spreading of the semidiurnal main mode between 130 km and 200 km. As can be seen in Figure 3, the transition region also produces a variation of phase with latitude that persists throughout the upper thermosphere. This variation amounts to about 90° of phase between $y = 0$ (the equator) and $y = 0.8$ (latitude = 53.2°).

The alteration of latitude structure within the transition region (130-200 km) is the most significant result of the spherical calculation. Although our artificial choice of dissipative processes precludes a direct association of calculated magnitudes with those that might be expected in the thermosphere, the calculated changes of latitude structure should be qualitatively indicative of what might happen in the real atmosphere. These changes are displayed in Figures 4a, b, c, and d where the variation of amplitudes (units arbitrary) and phase with latitude both below 100 km and above 200 km are shown for $\frac{\delta p}{p_o}$, u', v' and δT respectively. In the frictionless region both $\left|\frac{\delta p}{p_o}\right|$ and $|\delta T|$ have identical horizontal structures (Hough functions). Moreover, the latitude distribution of both is broadened in the transition region. However, the variation of phase with latitude (above 200 km) is greater for δT than for $\frac{\delta p}{p_o}$. The effect of the transition zone on the latitudinal structure of $|u|$ and $|v|$ is rather striking. Below the transition zone, the westerly velocity $|v|$, has a relative minimum at the equator; $|v|$ increases away from the equator to a maximum near 30° which is about 17% greater than the value at the equator and then decreases to zero at the poles. Above the transition zone, $|v|$ decreases monotonically away from the equator. The northerly velocity, which by symmetry is zero at the equator reaches a maximum near 40° below the transition, and near 30° above the transition zone. For all fields, there are no phase variations with latitude below the transition zone; above the transition zone the phases of semidiurnal oscillations at the equator lead those at 52° by 2 to 4 hours.

4. Implications for the thermosphere.

The preceding results show in detail how friction and rotation interact in an atmosphere where friction increases exponentially from an inconsequential value below 130 km to values which dominate atmospheric behavior above 250 km. While the specific model for friction (and thermal dissipation) is not realistic, the results give us insight into what is omitted when we adopt the equivalent gravity mode formalism. The effect of primary importance is the broadening of the latitudinal distributions of fields like pressure and temperature with the concommitent 30% decrease of oscillatory amplitudes in the equatorial thermosphere. Similar broadening may be expected to occur when friction is due to molecular viscosity. Thus in Lindzen (1971) the equivalent gravity mode formalism was used to predict a thermospheric semidiurnal temperature oscillation with an amplitude of 180°K or more at the equator; the present calculations suggest that calculations on a rotating sphere might predict amplitudes on the order of only 120°K. As already pointed out in Lindzen (1971), the latter value is still larger than what current observations suggest.

Similarly, the implication of the present calculations that one should observe a phase variation with latitude should hold for more realistic models of dissipation as well. Such behavior has obvious ramifications for the analysis of data -- which in some instances involves averaging over latitude, a procedure, which for phase variations on the order of those in Figure 4d, would lead to significant underestimates of semidiurnal amplitudes.

Finally, it should be added that the accuracy of the equivalent gravity mode formalism at the equator is within the limits suggested in Lindzen (1971). However, Figure 4 implies that away from the equator account must be taken of the variation of latitudinal structure.

Acknowledgements.

This research has been supported by the National Science Foundation under grant no. GA 25904 and by the National Aeronautics and Space Administration under grant no. NGR 14-001-193. We are grateful to the National Center for Atmospheric Research (supported by the NSF) for the use of their CDC-6600 computer.

References

Chapman, S. and R.S. Lindzen: Atmospheric Tides. D. Reidel Press, Dordrecht, Holland, 200 pp.

Lindzen, R.S.: Vertically propagating waves in an atmosphere with Newtonian cooling inversely proportional to density. Can. J. Phys., 46, 1835-1840.

Lindzen, R.S.: Internal gravity waves in atmospheres with realistic dissipation and temperature: Part I. Mathematical development and propagation of waves into the thermosphere. Geophys. Fluid Dyn., 1, 303-355.

Lindzen, R.S.: ________: Part III. Daily variations in the thermosphere. Geophys. Fluid Dyn., 2, 89-121.

Lindzen, R.S. and D. Blake: ________: Part II. Thermal tides excited below the mesopause. Geophys. Fluid Dyn., 2, 31-61.

Figure Legends

Fig. 1a. Amplitude of $\frac{\delta p}{p_o}$ for the main solar semidiurnal mode at the equator for equivalent gravity mode calculation (with dissipation), and rotating, spherical calculations with and without dissipation. (N. B. 21 pts. in latitudes have been used for higher accuracy in the spherical calculations shown.)

Fig. 1b. Same as 1a but for phase.

Fig. 2. Amplitude of $\frac{\delta p}{p_o}$ for the main solar semidiurnal mode at various latitudes (N. B. y = cos of latitude) for rotating, spherical calculation with dissipation.

Fig. 3. Same as 2 but for phase.

Fig. 4a. Amplitude (arbitrary units) and phase (arbitrary origin) of $\frac{\delta p}{p_o}$ as functions of latitude above 200 km (dashed) and below 100 km (solid).

Fig. 4b. Same as 4a but for u'.

Fig. 4c. Same as 4a but for v'.

Fig. 4d. Same as 4a but for δT.

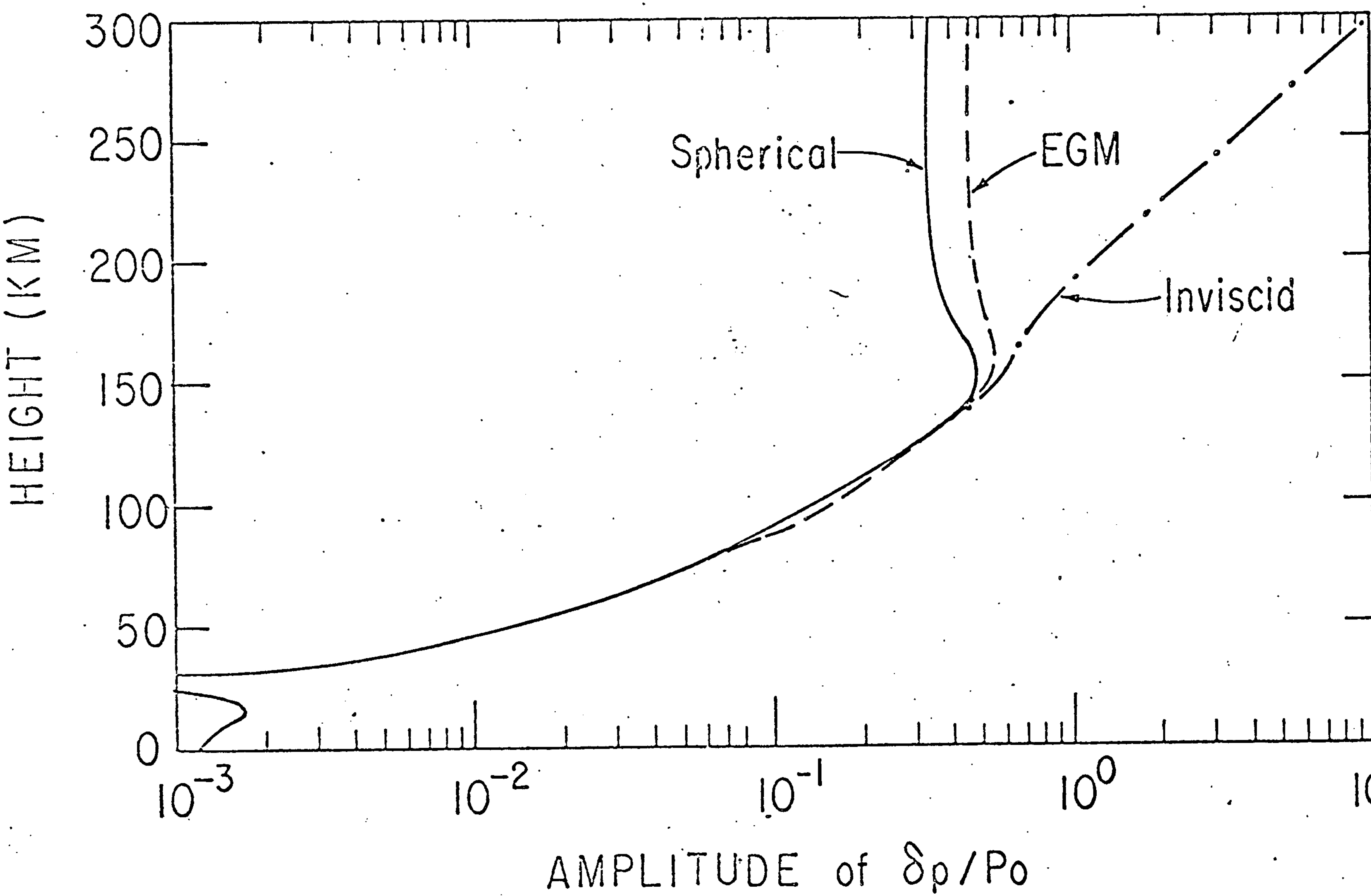
HEIGHT (KM)
300
250
200
150
100
50
0
Spherical
EGM
Inviscid
10^{-3}
10^{-2}
10^{-1}
10^{0}
10^{1}
AMPLITUDE of δp/Po

Fig. 1a

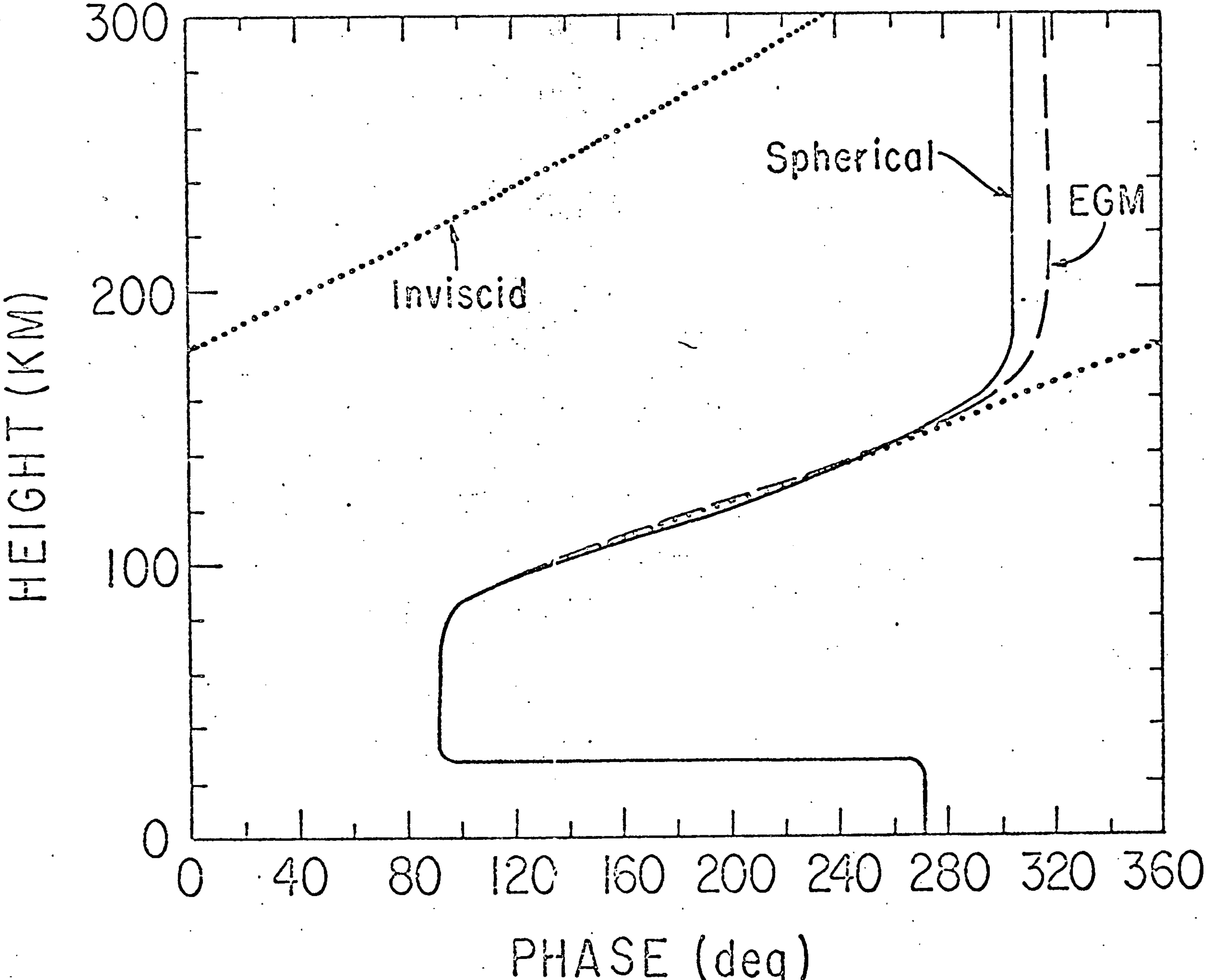

300
200
100
0
HEIGHT (KM)
0
40
80
120
160
200
240
280
320
360
PHASE (deg)
Inviscid
Spherical
EGM

Fig. 1b

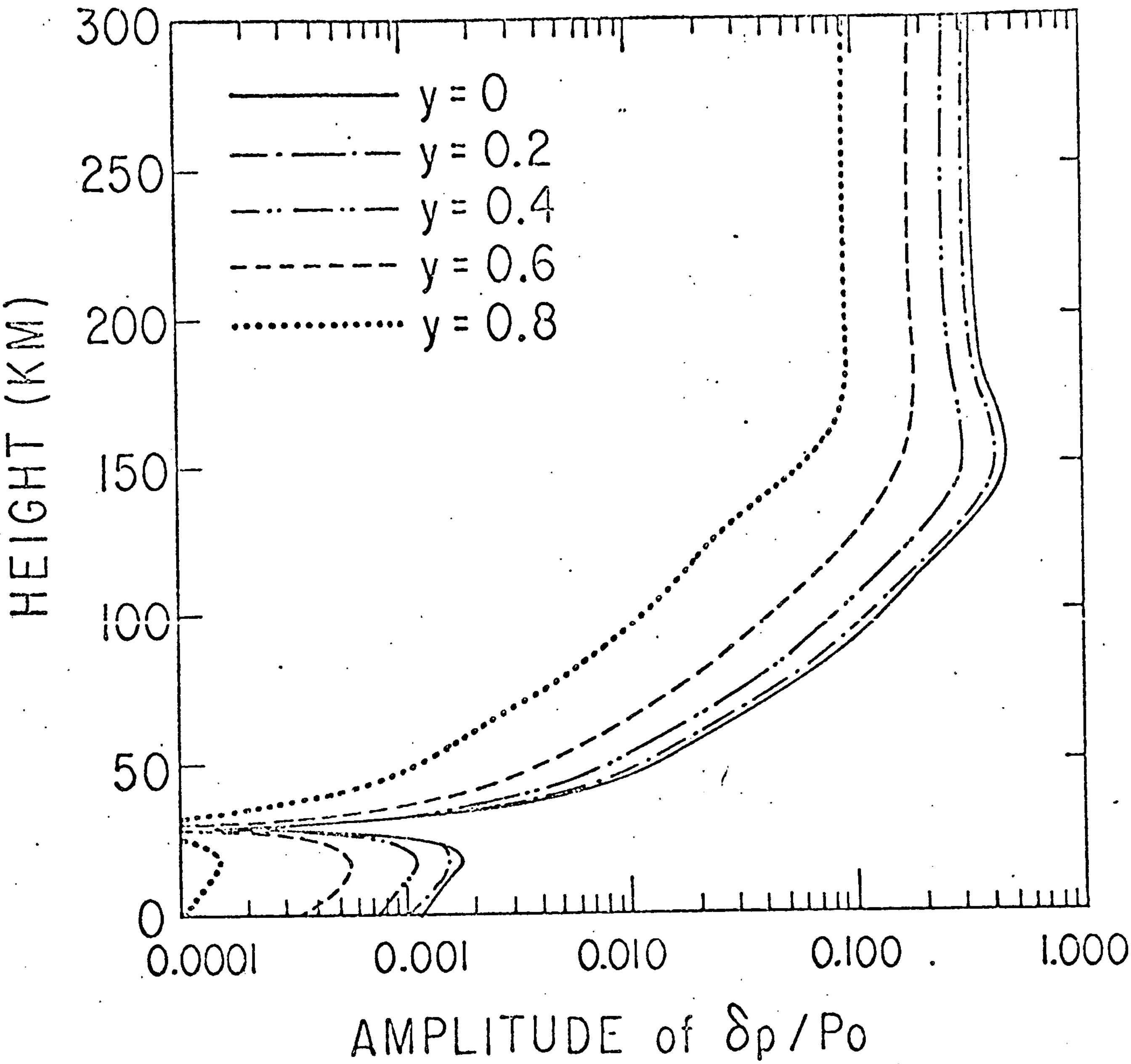

300
250
200
150
100
50
0
HEIGHT (KM)
y = 0
y = 0.2
y = 0.4
y = 0.6
y = 0.8
0.0001
0.001
0.010
0.100
1.000
AMPLITUDE of δp / Po

Fig. 2

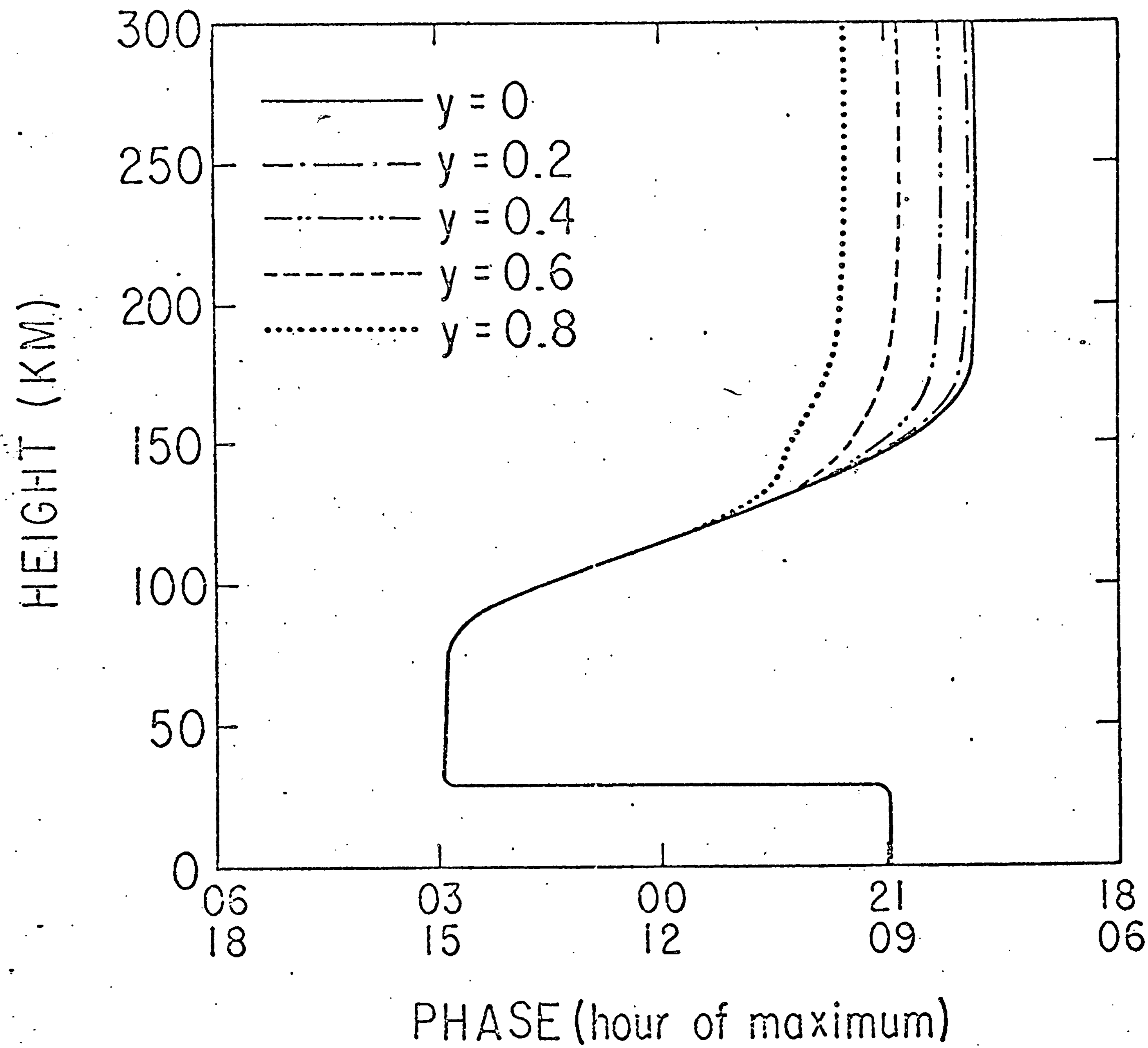

y = 0
y = 0.2
y = 0.4
y = 0.6
y = 0.8
HEIGHT (KM)
300
250
200
150
100
50
0
06 18
03 15
00 12
21 09
18 06
PHASE (hour of maximum)

Fig. 3

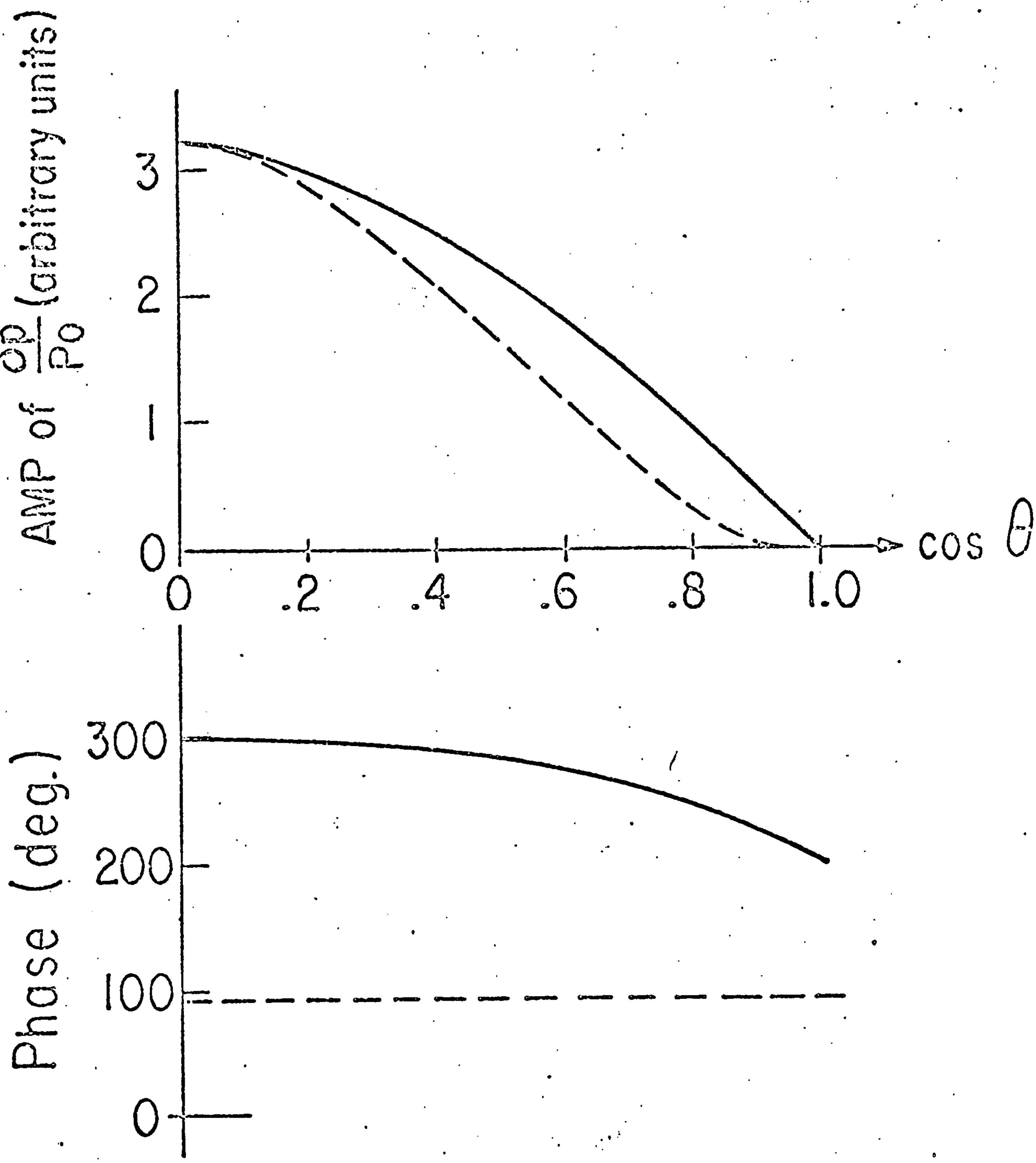
AMP of $\frac{\delta P}{P_0}$ (arbitrary units)
0
1
2
3
0
.2
.4
.6
.8
1.0
cos θ
Phase (deg.)
0
100
200
300

Fig. 4a

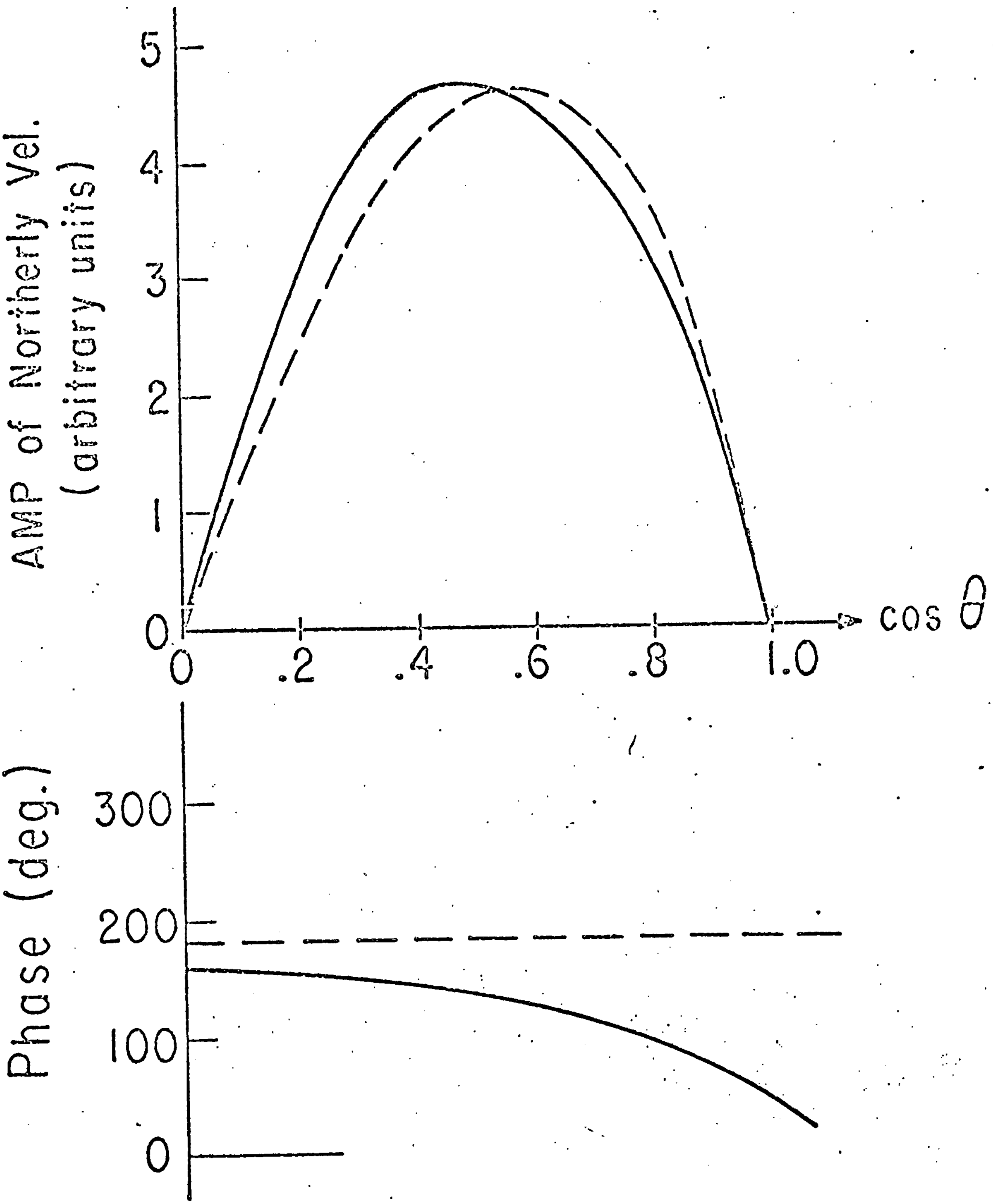
AMP of Northerly Vel.
(arbitrary units)
5
4
3
2
1
0
0
.2
.4
.6
.8
1.0
cos θ
Phase (deg.)
300
200
100
0

Fig. 4b

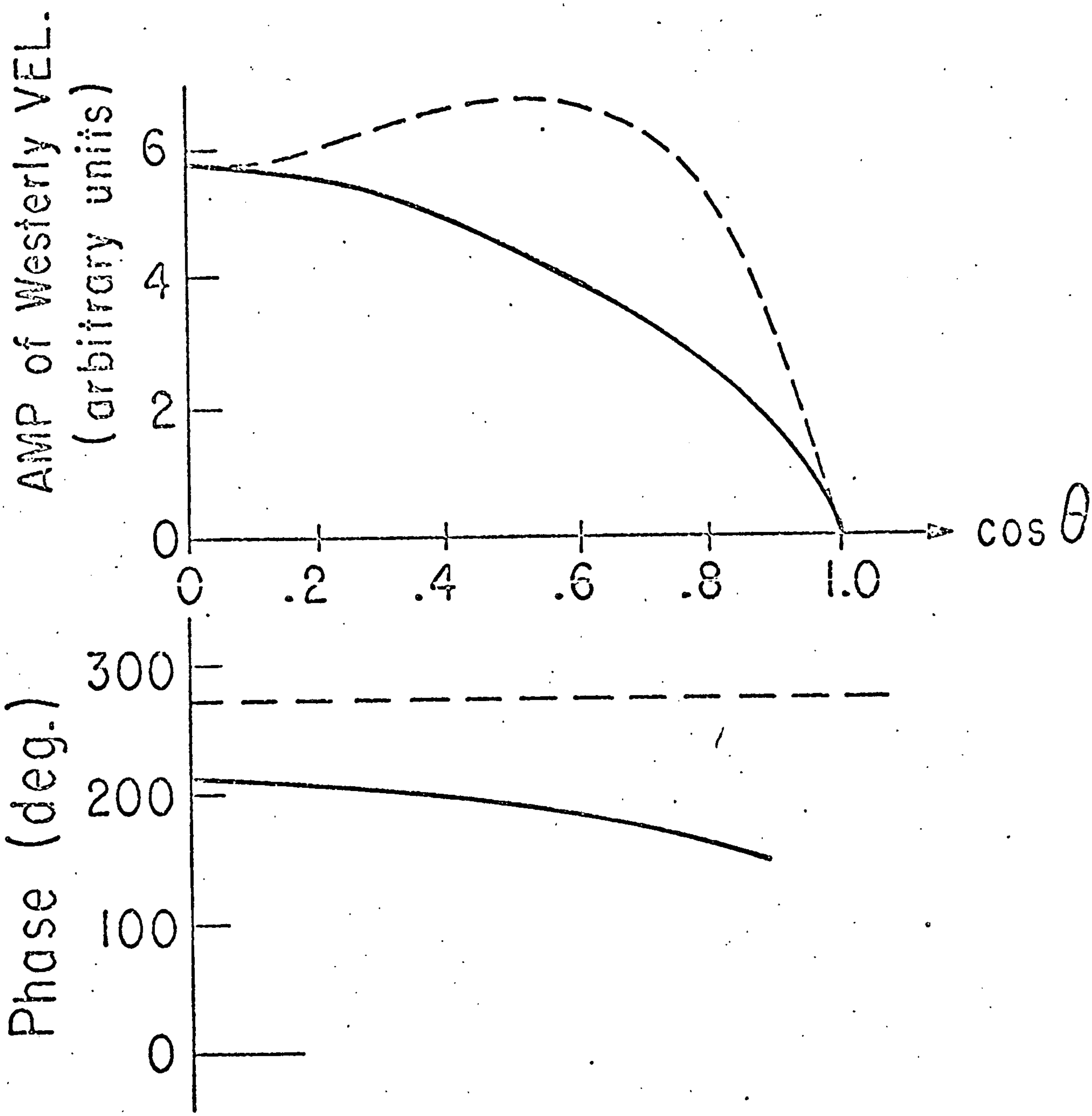
AMP of Westerly VEL.
(arbitrary units)
6
4
2
0
cos θ
0
.2
.4
.6
.8
1.0
Phase (deg.)
300
200
100
0

Fig. 4c

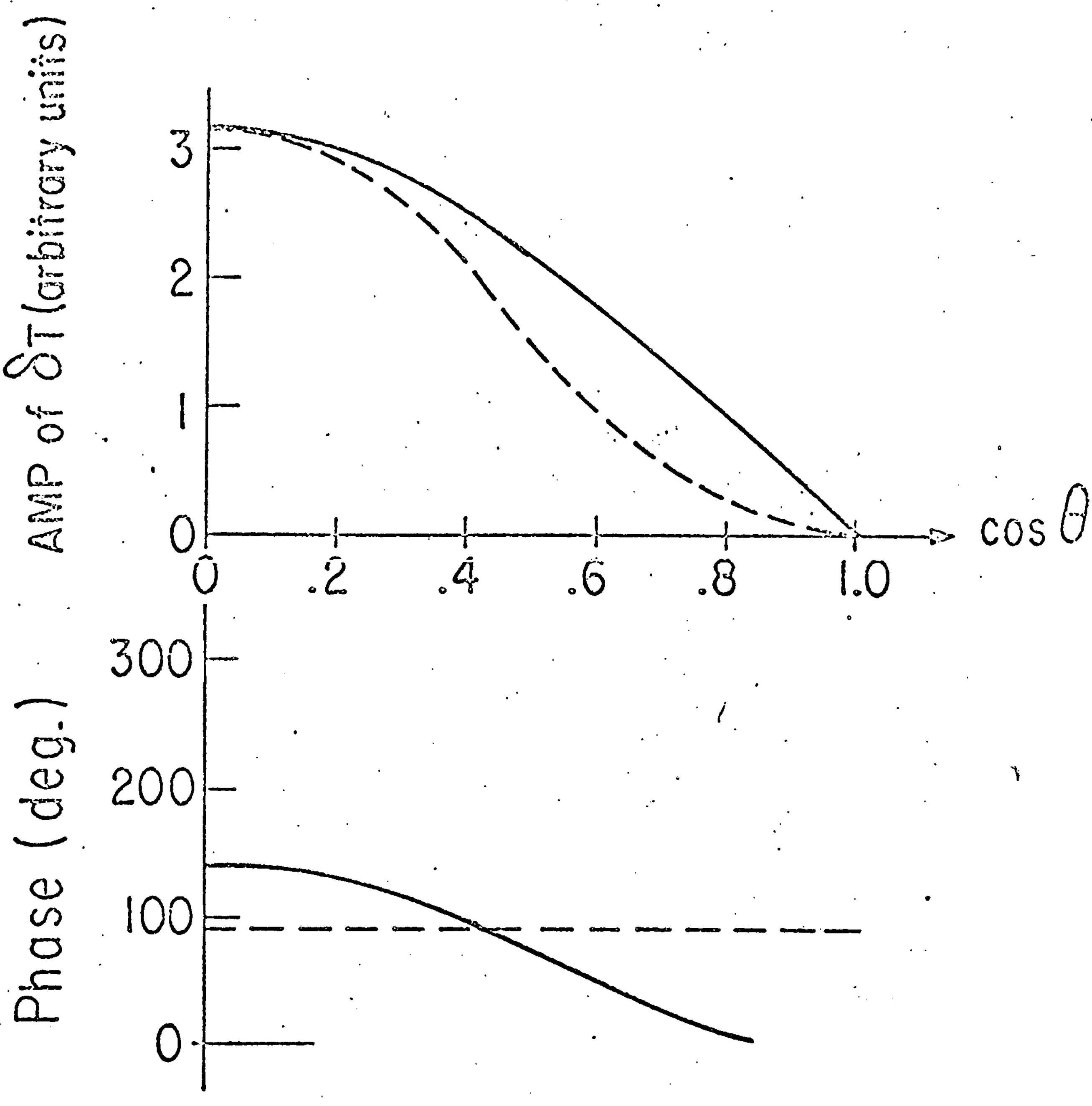
AMP of δT (arbitrary units)
3
2
1
0
0
.2
.4
.6
.8
1.0
cos θ
Phase (deg.)
300
200
100
0

Fig. 4d